ROYAL SOCIETY
OF CHEMISTRY

Check for updates

New framework of integrated electrocatalysis systems for nitrogen fixation

Qiuyang Lu,[a] Mingzi Sun [ID][a] and Bolong Huang [ID] *[abcd]

Nitrogen is one of the most essential molecules for daily life, especially as the utilization of nitrogen fertilizers prevents malnutrition. However, the generation of nitrogen fertilizers still relies on conventional chemical methods and exploring novel nitrogen conversion methods is of great significance. The electrochemical fixation method is a highly desirable approach due to its excellent production efficiency and lower environmental pollution. In this paper, we highlight the novel framework of integrated electrocatalysis systems for nitrogen fixation based on nanogenerators, as they are different from the typical nitrogen reduction reaction systems with a continuous high power supply. The novel hybridized and integrated nitrogen fixation system was demonstrated and introduced based on self-powered triboelectric nanogenerators (TENGs) as the power generator. Meanwhile, we also put forward distinct perspectives for enhancing the effectiveness of the hybridized system. This review will present advanced concepts for developing a next-generation nitrogen fixation system by integrating a TENG green energy harvester.

Introduction

Nitrogen is one of the most indispensable elements for life on Earth, but there is a significant difficulty in directly absorbing the molecule from the ambient environment. Although our

Dr Bolong Huang received his PhD in 2012 from University of Cambridge and his BSc in condensed matter physics from the Department of Physics of Peking University in 2007. Following a systematic training period as a post-doc in the Chemistry Department at Peking University and Hong Kong, in 2015, he started independent research at Hong Kong Polytechnic University and became a tenured Associate Professor in 2022. His main research interests focus on the electronic structures of nanomaterials, energy materials, solid functional materials, and rare earth materials, as well as their applications in multi-scale energy conversion and supply systems.

atmosphere contains 78% nitrogen gas and the ammonia synthesis reaction is thermodynamically exothermic, nitrogen fixation is problematic because of nitrogen's chemical inertness. At present, nitrogen fixation mainly relies on three methods: (a) atmospheric nitrogen fixation in geochemical processes,[1] which account for only 5 to 8% of fixation, (b) biological nitrogen fixation (BNF) performed by symbiotic and asymbiotic nitrogen-fixing microorganisms which serves as a vital reactive nitrogen (N_r) source in agriculture, and (c) industrial nitrogen fixation.[2,3] The limited production efficiency of the first two approaches makes them unsuitable to be the main N source for fertilizer. In order to accomplish a substantial conversion from naturally abundant nitrogen (N_2) into ammonia (NH_3), scientific and technical interest in the electrochemical nitrogen reduction process arose in the 19th century. In 1897, Lord Rayleigh created and advanced the basic concept of the industrial combination of nitrogen with oxygen using an electric arc. As of 1902, the work started to succeed with the increasing utilization of electricity generators; however, it was still not viable commercially.[4,5] At the same time, in 1895, another approach, which relied on the absorption of nitrogen by calcium carbide, was taken up by Adolph Frank and Nikodem Caro.[6] The cyanamide process was widely applied in a short time but was soon abandoned. The arc process and the Frank–Caro process[7] are both energy-intensive and

[a]Department of Applied Biology and Chemical Technology, The Hong Kong Polytechnic University, Hung Hom, Kowloon, Hong Kong SAR, China. E-mail: bhuang@polyu.edu.hk

[b]Beijing Institute of Nanoenergy and Nanosystems, Chinese Academy of Sciences, Beijing 100083, China

[c]Research Institute for Smart Energy (RISE), The Hong Kong Polytechnic University, Hung Hom, Kowloon, Hong Kong SAR, China

[d]Research Institute for Intelligent Wearable Systems (RI-IWEAR), The Hong Kong Polytechnic University, Hung Hom, Kowloon, Hong Kong SAR, China

inefficient. They were succeeded by the Haber–Bosch process, which rendered all previous methods obsolete. The Haber–Bosch process has been widely applied and commercially adopted for industrial nitrogen fixation. Up to 2010, more than 120 Tg(N) per year of N_r was fixed by this process with a sustainable rising trend.[8,9] As a result, in a space of ten years from 1995 to 2005, cereal production increased from 1897 to 2270 million tons and meat production increased from 207 to 260 million tons.[10] The fertilizer manufactured by this process can feed one-third of the population on earth.[11] Nevertheless, ammonia produced by the Haber–Bosch process is the most energy-intensive commodity chemical, requiring fossil fuels as feedstock and processing at high temperatures (300–500 °C) to account for 1–2% of global energy consumption.[12] Consequently, the fertilizer industries relying on the Haber–Bosch process are one of the largest greenhouse gas emitters, responsible for more than 1% of global anthropogenic CO_2 emissions.[13] All these disadvantages have led researchers to seek alternative, environmentally-friendly production methods.

Inspired by natural processes, photochemical and electrochemical nitrogen reduction has been investigated for more than 100 years because of its great benefits of sidestepping harsh conditions and intensive energy consumption.[14] By using solar energy or electricity as the driving force, N_2 molecules and abundant H_2O in the atmosphere can be utilized as nitrogen and proton sources, respectively. The reaction can be performed under mild conditions, which alleviates the problems of energy consumption and CO_2 emission.[3] However, the N_2 electroreduction process is still underexplored and its challenges are nonnegligible. Besides the generally concerning low selectivity of current electrocatalysts and low NH_3 yield rate, it is also severely challenged by the continuous energy supply and the characteristics of metal-based catalysts.[15] Present studies of electrocatalytic nitrogen reduction focus on various materials, from metals and metallic compounds (Cu, Pd, TiO_2) to non-metallic materials (black phosphorus).[16,98] Attention has also been drawn by multiple modification methods on the catalyst surfaces, for instance, modifying the nanoparticle surface with oxygen-rich tannic acid[17,18] or introducing metal–sulfur linkages to strengthen the adsorption of N_2 intermediates on the surface.[19,20] Although great efforts have been dedicated to improving the yield of ammonia *via* photochemical and electrochemical nitrogen reduction methods, the current insufficiency keeps them from replacing the conventional Haber–Bosch process.

The triboelectric nanogenerator (TENG) is a burgeoning energy-harvesting strategy that is a pioneering method of collecting energy from ambient mechanical movements. The TENG originates from Maxwell's displacement current and was first invented in 2012.[21,22] It exhibits a compelling ability to harvest and convert mechanical energy into electrical energy, especially from irregular mechanical energy and low-frequency energy. Its intrinsic characteristics of continuous output and high voltage make researchers cautiously optimistic about the TENG energy source. Also, the manufacture of TENG devices features low-cost and abundant material sources. This energy-saving and eco-friendly method holds great promise for

developing a self-powered and sustainable nitrogen fixation system. In addition to harvesting mechanical energy from natural sources, such as wind and water flow, it is also feasible to reuse the residual kinetic energy of exhaust gases or wastewater.[23]

A TENG device often is composed of two dissimilar materials, electrodes and external loading circuits. When the two surfaces come into physical contact, electrostatic charges redistribute on the interface. A potential drop is built up when the two surfaces separate and the electron flow is driven by the potential difference between the electrodes on the backs of the two contact objects. For nitrogen fixation, although molecular N_2 is abundant in the ambient environment, the inevitable problem is that breaking the highly stable N≡N triple bond (940.95 kJ mol^{-1}) under mild conditions (room temperature and ambient pressure) requires high energy. However, the TENGs generally produce a high voltage that is capable of breaking the stable covalent bond. In addition to driving microplasma discharge devices for nitrogen dissociation and nitrogen oxide formation, a TENG can also function in a dual mode to supply another independent electrocatalytic cell for ammonia synthesis. The broad prospects and wide range of application scenarios for TENG add a new and rapidly changing dimension for a self-powered nitrogen fixation system that fulfills the growing prevalence of N_r consumption.

In this perspective, we present several studies based on hybridized TENGs with nitrogen reduction cells for nitrogen fixation. In combination with TENGs manufactured and triggered by distinct methods, a fundamental nitrogen fixation system with an explicit energy supplier is demonstrated. We also focus on a wide variety of improvement approaches in terms of TENG output and electroreduction performance. The recent advances increase the investigation range and challenge the Haber–Bosch process in the aspects of simultaneously reducing energy consumption and expanding power sources. This research also benefits the construction of sustainable distributed fertilizer synthesis systems in developing countries to relieve agricultural production deficiencies. Appropriate concepts and innovative integrations are proposed for improvement of the hybridized TENG and nitrogen fixation system.

Fundamental working modes and output performance of TENGs

The awareness of triboelectrification goes back to ancient Greek times; however, people usually see it as a negative effect of normal life or industrial activities. After the invention of TENGs, researchers began to learn about the effect and utilized the coupling of triboelectrification and electrostatic induction to convert mechanical energy into electricity. The preliminary working mode of a TENG is the contact-separation mode. The vertical contact-separation mode requires two dielectric films with at least one made of insulative materials. Once the two films come into contact, opposite charges are redistributed on the two surfaces due to distinct electron affinity. The removal of

This journal is © The Royal Society of Chemistry 2022

J. Mater. Chem. A, 2022, **10**, 19506–19517 | **19507**

the external mechanical force separates the surfaces and creates a potential drop between the electrodes anchored on the back of the two dielectric films. If the two electrodes are connected in an external circuit, electrons flow from one to the other to balance the electrostatic field. With further contact, the potential drop is eliminated and the induced electrons flow back. The periodic movements of the two dielectric films drive electrons to migrate back and forth, resulting in an alternating current (AC) in the external circuit. The other well-established TENG working mode is the free-standing mode, which requires a pair of symmetrical electrodes underneath two separated dielectric layers, with the electrodes and layers being the same size. The moving object and the dielectric layers are pre-charged and electrons remain on the surfaces. The movements of the objects between the two electrodes creates an asymmetric charge distribution and a current flow in the electrically connected electrodes. In addition to these two widely employed modes, single-electrode mode and in-plane sliding mode are also fundamental working modes of TENGs, but practical applications based on these two modes are relatively rare.

The goal of TENG applications is to collect ambient mechanical energies that are generally neglected or wasted in daily life. TENGs can convert irregular and low-frequency motions from humans and nature into electricity. The energy created by human motion can directly serve as a portable energy supply or be stored by a battery.[24,25] For large-scale energy harvesting of hydropower, a TENG is much more effective than an electromagnetic generator (EMG) in the low-frequency range (<5 Hz) which is more comparable to natural conditions.[26] Additionally, EMGs are high-quality infrastructure and often costs lots of time for construction; in contrast, the advantages of TENGs are their low cost, ease of manufacturing, and diversity in choices of materials. TENGs are also capable of harvesting large-scale energy, more than 1 MW km$^{-1,2}$ using integrated network configurations.[27] TENGs can achieve a maximum high open-circuit voltage of more than 2103 V,[28] but the current is low[29] when it functions as a single unit (<420 µA). The low current characteristic can be utilized to obtain a higher conversion efficiency in nitrogen reduction, making TENGs suitable for electrochemical nitrogen fixation.[30]

Key concepts and preliminary design

Global ammonia consumption was estimated to have reached 150 million metric tons by 2017.[31] Currently, the Haber–Bosch process is one of the largest energy consumers in terms of fossil fuels, which leads to a false optimization that does not reduce carbon emissions.[32] In the last decades, studies on TENG design and modification strategies have attracted a lot of interest for sustainable and renewable energy harvesting from a variety of mechanical energy sources, such as human motion,[33,34] wind,[35,36] and water flow.[27,37] At the same time, the generated electricity can be employed for self-powered electronic devices. Their vast energy sources and constant production also endow TENGs with splendid properties to support effective N_2 electroreduction. Wong *et al.* present a preliminary integrated system, a TENG device capable of 1300 V output voltage, with

a micro-plasma discharge reactor connected as the external electronic device. The TENG-driven reactor opens unprecedented opportunities for a carbon-free nitrogen fixation strategy. It is important to understand the previous configuration for the purposes of subsequent evaluation. The integrated system is illustrated in Fig. 1.[38]

The TENG component in this system functions purely as an energy source; in other words, the nitrogen fixation device is separate from the TENG (Fig. 1a and b). Owing to its simple configuration and manufacturing process, this design has inspired multiple variations. The configuration of the TENG device is rather simple and it is easy to manufacture or alter because it functions in a contact-separation mode. The TENG section is composed of a polyurethane (PU) foam and an ebonite sheet as the contact layers and two nickel (Ni) electrodes are adhered on the backs of the two contact surfaces. Polycarbonate is utilized as the substrate (Fig. 1c). The micro-plasma discharge reactor is an air-filled transparent cylinder in which the two steel needles work as the discharge electrodes and are directly connected to the Ni electrodes. Therefore, the generated potential difference can serve as the energy source for air discharge in the cylinder. To absorb the generated nitrogen oxide, a layer of deionized (DI) water is placed on the bottom of the discharge device. With a periodic force of 70 Newton (N), the two surfaces are negatively or positively charged based on their affinities to polarization and create an electron flow in the external circuit (Fig. 1d). With the next suppression, the current reverses to re-build the polarization on the interface. Subsequently, an alternating current (AC) corresponding to the
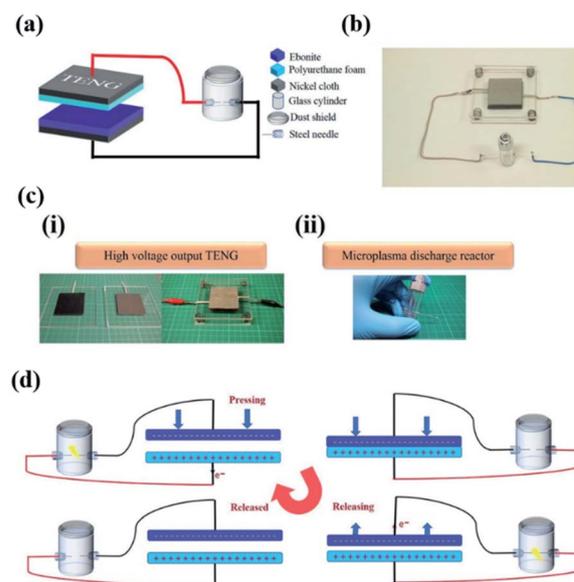

Fig. 1 Illustration of the hybridized TENG and the micro-plasma discharge system. (a) Schematic and (b) real pictures of the integrated nitrogen fixation system. (c) Real pictures of the (i) TENG and (ii) micro-plasma discharge reactor. (d) Schematic diagram of the working mechanism of the TENG and the energy supply to the micro-plasma nitrogen fixation system. Reproduced with permission.[33] Copyright 2019, Wiley VCH.

19508 | *J. Mater. Chem. A*, 2022, **10**, 19506–19517

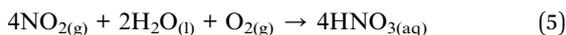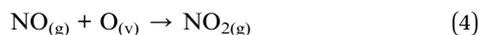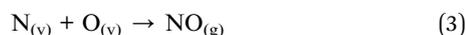This journal is © The Royal Society of Chemistry 2022

triggering frequency is created. The voltage and current are applied to the steel needles at the interior of the cylinder with a gap distance of 0.2 mm. Once the voltage exceeds the dielectric strength of air, ionization of air molecules and micro-plasm discharges occur in the gap between the two needles.

Due to the continuous energy supply from the TENG device, the charges remaining on the two needles aggregate and the discharge phenomenon intensively occurs in the positive half cycles with an average released energy of 0.26 μJ. However, the distance between the discharge needles has shown great influence on the reaction quality and so the researchers also assessed the effect of the variation of distance. When the distance was changed to 0.6 mm in value, the amounts of discharge decreased to about 0.3 times the initial value per operation cycle. Besides the efficiency decline, the discharge current is reduced to 287 μA with a voltage increase to 2 kV. The researchers suggested that a longer distance creates harsher conditions to realize air breakdown and form a conductive path. The experiment demonstrated the improvement of higher voltage coupled with reduced current and charge number when increasing the distance to 0.6 mm. In order to optimize the discharge efficiency by choosing a suitable distance, the dependencies between the gap distance and discharge voltage, current, and average released energies were investigated using distances of 0.2 mm to 0.9 mm. The results show that 0.3 mm is preferable and exhibits optimized micro-plasma discharge with the average released energy reaching 0.28 μJ.

In the experimental design, nitrogen reduction with an atmospheric air source is operated without an H-cell. Within this process, nitrogen in the air is dissociated and converted into nitrogen oxides. Relying on a high electric field with potential accumulation, the strong discharge strength causes direct activation of nitrogen and oxygen atoms in the interior of the glass cylinder. These activated atoms can be dissociated into free radicals, as in the following examples.

$$O_{2(g)} + e^- \rightarrow 2O_{(v)} + e^- \tag{1}$$

$$N_{2(g)} + e^- \rightarrow 2N_{(v)} + e^- \tag{2}$$
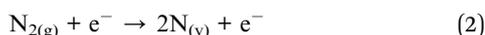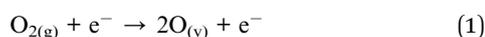
The free radicals can further react with each other and synthesize nitrogen oxides. They then further react with the deionized water, forming nitric acid on the bottom of the reaction device.

$$N_{(v)} + O_{(v)} \rightarrow NO_{(g)} \tag{3}$$

$$NO_{(g)} + O_{(v)} \rightarrow NO_{2(g)} \tag{4}$$

$$4NO_{2(g)} + 2H_2O_{(l)} + O_{2(g)} \rightarrow 4HNO_{3(aq)} \tag{5}$$

$$3NO_{2(g)} + H_2O_{(l)} \rightarrow 2HNO_{3(aq)} + NO_{(g)} \tag{6}$$

To identify the production reliability and efficiency, the work conducted a series of assessments. First, the emission spectrum proved the existence of dinitrogen and nitrogen-free radicals, which provides strong evidence of successful dissociation. The concentrations of nitrogen dioxide (NO_2) and nitrate were also examined while varying the distance from the reactor to the detector inside the cylinder. The negative relation revealed the ongoing reaction and diffusion process. The maximum production effectiveness of this device is about 250 ppm of nitrate after operating for 400 minutes. Compared with the yield of the industrial Haber–Bosch process (37.1 MJ mol^{-1}), it exhibits an obvious shortcoming in production ability. However, the TENG is a sustainable and renewable energy harvester with abundant methods to improve its functional strength. With goal-oriented modifications and optimization, the efficiency of the TENG hybridized nitrogen fixation system can be further improved.

General fabrication and modification of TENGs

The 25 cm^2 size of the PU foam and ebonite sheet was standardized for the performance evaluation. When a single TENG functions under a periodic trigger, the open-circuit voltage (V_{OC}) and the short-circuit current (I_{SC}) can reach 1300 V and 60 μA, respectively. The maximum instantaneous power is capable of reaching 27 mW when the external circuit employs a loading resistance of 100 MΩ.[38]

The results and working mechanism of the TENG reveal that the energy value is highly dependent on the surface properties and external loading resistance. In the search for continuous and high voltage output, multiple modifications and optimizations have been derived from the preliminary system. As is known, the potential difference created between two different surfaces hinges on the surfaces' ability to gain or lose electrons. Consequently, many material recombinations and surface modifications have emerged over the last few years and their enhancements on triboelectric energy harvesting ability are introduced here.

Material choices for TENGs

To achieve an ideal TENG output voltage, the potential difference between the two selected materials needs to be sufficiently large. Surface affinity for negative or positive charges is the essential intrinsic property of possible materials and this standard restricts the selection of TENG counterparts. Generally, the material choice is based on existing triboelectric sequences or experimental results. As concluded by Zhang's work, the most used materials for negatively charged surfaces are polytetrafluoroethylene (PTFE),[39–42] polydimethyl-siloxane (PDMS),[43–45] fluorinated ethylene propylene (FEP),[26,46,47] and Kapton.[48] Polyvinylidene fluoride (PVDF),[49] polyolefin,[50] polystyrene (PS)[51] and graphene[52] also have a wide variety of applications.[53] On the other hand, the range of preferred positively charged materials is also extensive. Al,[54] Cu[55] and Au[56] are the top choices in metals while nylon,[57] cellulose[58] and latex[46] are typical selections for multiple counterparts. The hybridized TENG and solar cell systems often employ indium-tin-oxide (ITO) as the surface material for its transparent appearance.[36,59] Except for a unique choice for a specific purpose, the

This journal is © The Royal Society of Chemistry 2022

J. Mater. Chem. A, 2022, **10**, 19506–19517 | **19509**

choice of triboelectric pairs is usually influenced by the synthesis method, durability, availability, *etc.*

Surface engineering

In addition to appropriate material choices, surface texture and carving can also manipulate the total output performance without changing the elementary structure. Compared with a flat surface, an enlarged output performance can be realized by introducing a micro-/nano-carved morphology on the surface to sufficiently increase the contact area.[60–62] The output power density can be improved to at least two times larger that of the flat surface. The laser-assisted surface manufacturing method is a facile technique with great flexibility.[61] Direct surface growing is another general means to improve the output performance.[63]

Structure optimization and integrated nitrogen fixation system

In order to further increase the energy production efficiency on a large scale, multiple-layer structures and repeated units are of great interest. Combined with 3D printing technology, this type of TENG is capable of customized design and the output power density varies from 1.48 to 6.7 W m^{-2}.[64] This fabrication utilizes a thermoplastic elastomer (TPE) filament and a polylactic acid (PLA) filament as the fundamental soft and hard materials, respectively. The report exhibits three distinct kinds of TENGs with their geometrical structures changing from simple to complex. Their open-circuit voltages vary from 410 to 2360 V, which extremely exceeds the value of the previously mentioned device with a regular voltage of 1300 V. In addition to the V_{OC}, the output current I_{SC} also increases from 420 μA to 1.7 mA.

In this work, researchers chose the multi-layer asway triboelectric nanogenerator (PMLA-TENG) as the energy supplier for their self-powered nitrogen fixation device, as illustrated in Fig. 2a. The PMLA-TENG is fabricated with the PLA filament hard material and a basic fan-like structure is utilized to assemble multi-layer TENGs. The operation mode is to convert a rotating mechanical force into swinging movement *via* a crank-rocker mechanism. Fig. 2b shows the potential distribution of the TENG device at different deflection angles; it clearly exhibits a circular pattern. When applying an external force, driven by water or another common ambient mechanical force, the rocker mechanism is triggered by the crank mechanism. Then, the swingable circumferential substrate starts a reciprocating movement inside of the fixed substrate. On each interface, a general contact-separation mode is created due to the periodic movement. The output performances of the integrated TENG are depicted in Fig. 2c–h at working frequencies of 2–5 Hz. The results obviously show a positive relationship between the number of friction layers and output current I_{SC}. In contrast, the V_{OC} does not exhibit a strong increase because of the parallel-connected circuit. The maximum instantaneous power density can reach 6.7 W m^{-2} at a loading resistance of 1 MΩ. For the nitrogen reduction process, a melamine-sponge-covered carbon paper is utilized as the discharge electrode and a graphite rod is employed as the other one. The nitrogen electroreduction is performed in 0.1 mol L^{-1} HCl which was
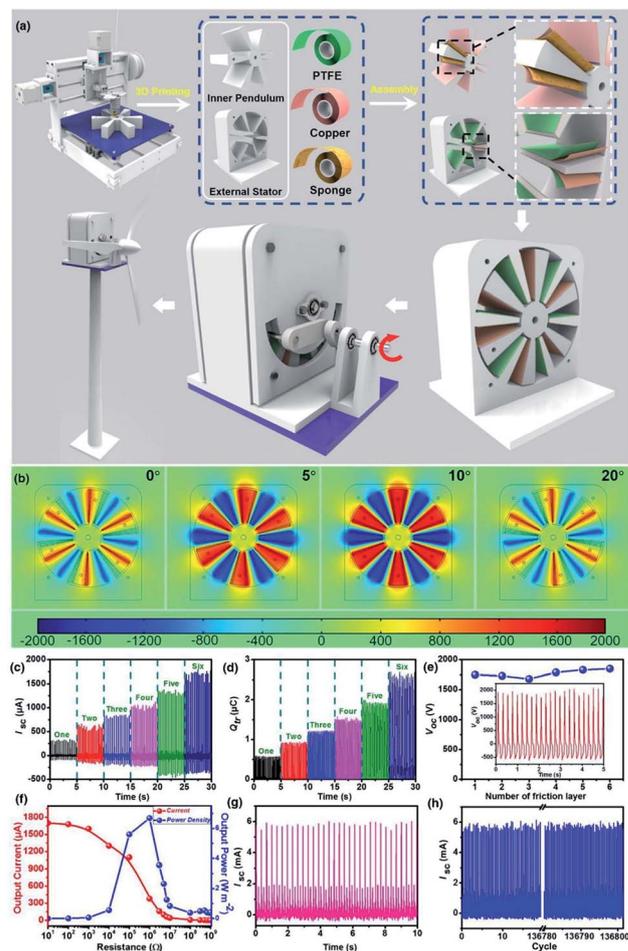

Fig. 2 (a) The schematic structure and fabrication process of the PMLA-TENG. (b) The potential distributions of different angles simulated by COMSOL. Functional parameters (c) ISC, (d) Qtr, and (e) VOC of the PMLA-TENG with different pairs of friction layers. (f) The relationship between the loading resistance, instantaneous current and power density of the TENG with six friction layers. (g) ISC after processing by a transformer and a rectifier. (h) The ISC processed by a transformer and a rectifier after about 136 800 cycles (working continuously for 6 h). Reproduced with permission.[59] Copyright 2019, Elsevier.

purged with N$_2$ for at least 30 minutes before assessment. Spectrophotometrical estimation of the production of NH$_3$ and N$_2$H$_4$ reveals that the nitrogen reduction occurs in the voltage range from 5 to 25 V and an instantaneous peak value of 36.41 μg h^{-1} mg$_{cat}$$^{-1}$ can be achieved when the device is applied at 15 V voltage.

Another structural optimization was reported by Wang *et al.*, in which a dual-TENG self-powered device was assembled to enable the non-noble-metal electrocatalytic reduction of nitrogen.[65] The structural diagram is illustrated in Fig. 3a and the working mechanisms of the TENG and nitrogen fixation system are shown in Fig. 3b and c. The nitrogen fixation system and the downstream ammonia synthesis device are both powered by the same TENG device. The integrated TENG-supported system uses the air discharge induced by the high voltage from
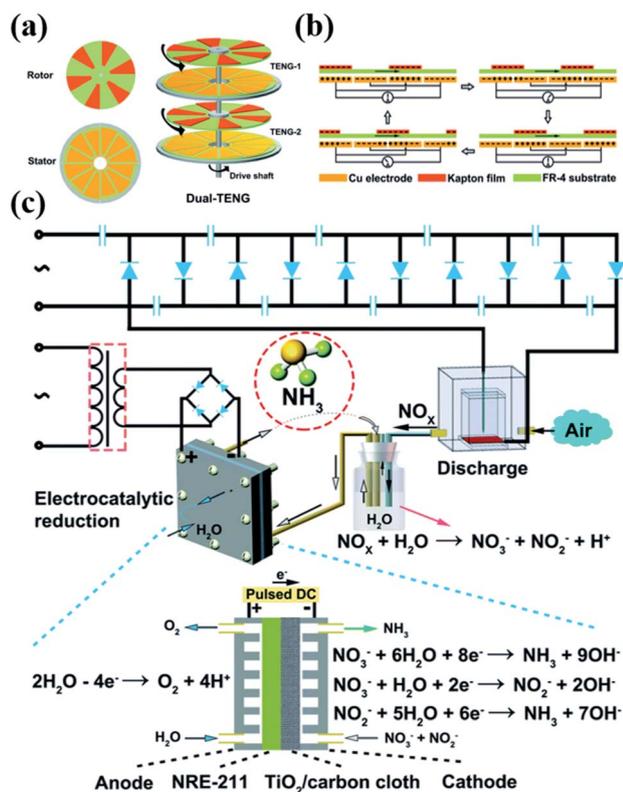
Fig. 3 Schematic diagram of TENG and nitrogen reduction process. Schematic diagram of the dual-TENG. (a) Rotor and stator of the dual-TENG and its construction. (b) Working principle of the TENG. (c) Ammonia synthesis devices. Reproduced with permission.[60] Copyright 2020, Royal Society of Chemistry.

the Kapton surface is loaded with negative charges by rubbing with Cu film. The configuration indicates the distinctive working mechanism and the applicable environments of the contact-separation mode and the sliding mode. Also, compared with the aforementioned structures, TENGs with a sliding mode are typically more lightweight and flexible, which realizes easy fabrication.

The question of whether the separation leads to a reduction in TENG energy scavenging has also attracted enormous interest. In 2014, Wang *et al.* compared five different modes with contact and non-contact sample devices for their total performance.[66] Through pre-triboelectrification, the FEP layer can generate electricity by swinging between two connected electrodes because the electrons can be preserved on the insulative surface for hours. The reason for developing a non-contact mode is that a real application of TENGs generally requires an external force, such as a tangential force in the sliding mode. Therefore, a steady input of mechanical force is desired to keep good in-plane contact with the TENG interface. Due to the unavoidable imprecision of manufactured machines and possible irregularities of ambient mechanical triggers, a stable input force can be hard to sustain. Thus, a good tolerance of separation space is crucial for practical TENG devices to expand their durability and constant working ability.

In the disk-structure TENG, the working mechanism is fundamentally similar to the parallel sliding device. When the rotor is driven by the shaft, the negatively charged Kapton first overlaps with one of the paired Cu film electrodes. Since the Kapton film has a negative charge, the electrostatic effect induces a positive charge accumulation on the opposite Cu electrode to achieve electrical equilibrium. After the potential difference is fully compensated by electron migration, the rotor starts to slide. During rotation, the Kapton film gradually decreases its cover area of the first electrode accompanied by an increase of the second electrode proportion. As the rotor moves, the positive charges gradually shift with the negatively charged area, which induces a current flow. With continuous sliding, the Kapton film fully overlaps the second electrode and reverse current flow starts to occur. Since all the electrodes are connected in parallel, the produced current has an AC profile. A complete cycle of this sliding freestanding non-contact TENG is from the overlapping of one of the Cu electrodes in the first pair to the same-position electrode in the second pair. For a higher voltage output, a ten-stage multiplier is connected. The discharge device is also based on a needle-plate structure. When applying a strong voltage after the multiplier enlargement, intense nitrogen and oxygen dissociation occurs and the produced nitrogen oxide flows in the injected air source. The continuous airflow not only provides sustainable reaction materials but also brings the nitrogen oxides into the gas-washing equipment. There, the nitrogen oxides sufficiently react with water and produce electrolytes containing NO_3^- and NO_2^-. To further assist the nitrogen fixation, the subsequent electrocatalytic reduction to produce ammonia is also included in the system. The electrocatalytic process is powered by the TENG-2 with a transformer and a rectifier, which can transform

the TENG to first fix N_2 and oxygen into NO_x. Then, the subsequent nitrogen fixation assisting section washes the gas flow of NO_x with water and applies an electrochemical cell with TiO_2 as the catalyst to directly convert NO^{3-} and NO^{2-} to NH_3. Specifically, the working mechanism of this TENG is the freestanding sliding mode, which is fundamentally different than the aforementioned contact-separation mode. In order to reduce friction damage to the contact surface, this design takes advantage of the non-contact freestanding mode with a proficient application of electrostatic induction effects. The simultaneous dual-TENG systems can effectively drive electrocatalytic reduction to generate ammonia in an electrochemical cell. With a NO_x gas flow of 3.5 m^3 min^{-1}, the ammonia yield can reach 2.4 μg h^{-1} in the self-powered electrocatalytic system with a TENG at room temperature and atmospheric pressure.

Two disk-structure substrates are vertically assembled on a steady drive shaft with a small distance between the two layers. The fixed slice is a PCB circuit board anchored with 6 pairs of Cu electrodes in parallel connection where each pair serves as a pair of corresponding electrodes for the rotation slice. Six separate Kapton films are deposited on a subtracted epoxy glass cloth board (FR-4), a pressed insulative material. The FR-4 thickness of 0.3 mm is selected to reduce the rotational inertia. To achieve considerable electrostatic induction,

This journal is © The Royal Society of Chemistry 2022

J. Mater. Chem. A, 2022, **10**, 19506–19517 | **19511**

the AC current to direct current (DC). With the pulsed DC power, NO_3^- and NO_2^- are further reduced to NH_3.

Independent electrocatalytic reactor

The difference between the first contact-separation TENG with a micro-plasma discharge reactor and the dual-TENG device is not only the isolated electrocatalytic reaction cell. The function mechanism and the modification are also different due to the distinctive improvement strategies. The thin FR-4 substrate is difficult to keep horizontally oriented and unwanted friction leads to electron neutralization. This reduces the potential difference in the interface and the open-circuit voltage of the dual-TENGs reaches 630–720 V. The transferred charges and short-circuit current increase with rotation speed and achieve a high performance of 1 μC and 0.55 mA at the speed of 5000 rpm. The output voltage is still not high enough to exceed that of the previously mentioned work, which shows a high voltage performance of more than 1000 V. However, by applying a ten-stage voltage multiplier circuit, which contains four kinds of high-voltage resistive capacitors and diodes, the voltage can be boosted to about 7 kV.

The most common discharge device is composed of two steel needles, but, as the energy supply is changed to DC, a steel needle coupled with a tantalum sheet is utilized. The electrodes can be determined as negative or positive electrodes according to the direction of the DC. Since the AC-type current enables a reversible energy supply between the two needles, a difference between the negatively charged and positively charged electrode cannot be demonstrated. By changing the bias between the needle-sheet reactor, researchers observed enhanced production of nitrogen oxides when the needle was applied with a negative bias. Additionally, the inlet airflow brings the generated nitrogen oxides into a gas-washing bottom layer with DI water and the concentrations of dissolved NO_3^- and NO_2^- were detected when the applied bias changes. The results suggest that when a positively charged needle operates, NO_3^- and NO_2^- show similar concentrations of less than 1 mg L^{-1} in the water. However, the concentration of NO_3^- reaches 7.4 mg L^{-1} with a negatively charged needle electrode. In contrast, NO_2^- only shows a negligible concentration of less than 0.02 mg L^{-1}. According to this result, applying negative potential on the steel needle is preferred.

Reactor modification

To improve the efficiency of the electrocatalytic process, a commercial nano-TiO_2 (P25) is employed as the new catalyst. TiO_2 is considered to be a low-cost and effective catalyst for nitrate and nitrite reduction. The novel electrocatalytic pair is composed of a carbon cloth covered by TiO_2 nanoparticles and a graphite electrode (Fig. 4a and b). Compared with naked carbon cloth, the TiO_2 modified electrode exhibits considerable improvement (Fig. 4c) in the reduction in the standard KNO_3 solution when driven by DC power (−3 V) for 6 h. The concentration of NO_2^- is also tested to verify the utility of the catalyst. The NO_2^- concentration is much lower when TiO_2 is present. The reduction efficiency when directly using the KNO_2 solution

also shows better performance when the electrode is decorated. To achieve a better yield rate, the researchers also incorporated an electromagnetic transformer. As is known, when the voltage is settled, a larger current leads to better effectiveness. The optimal transformer ratio is selected to be 350 : 12 and the performances with or without the electromagnetic transformer are shown in Fig. 4d and e. The results illustrate a strong improvement of the NH_3 yield with the help of the transformer. A yield of 20.8 μg h^{-1} and an efficiency of 13.9% of the TENG-2 can be achieved. However, when the current is increased to a milliampere level, severe anodic corrosion occurs, which limits the further improvement and constant operation of the electrocatalytic reactor. To solve this problem, researchers introduced a dual-compartment electrochemical cell, as shown in Fig. 4f. With this component, they conducted an all-around evaluation of the functional characteristics of the dual-TENG nitrogen fixation devices. Fig. 4g exhibits the concentration and mass yield after 1 h of reaction. The dual compartment cell demonstrated that the separate configuration enables the improved efficiency and consistent stability of the system.

Hybridized system with TENG

TENGs have been widely employed in multiple atmospheres for their strong adaptability, low cost, easy fabrication, and excellent conversion efficiency. In scavenging applications for nitrogen fixation, the researchers have to take both the availability of external forces and the scale of output values into consideration. In order to enhance the working efficiency of TENGs, we also reviewed the studies regarding how to get high-efficiency output and suitable integration of several functional cells; the general similarity can be described as choosing suitable energy sources and comparable configuration designs. As mentioned, for contact-separation mode, a reciprocating vertical force is required and, therefore, a freestanding sliding mode typically needs a tangential force. Discovering a method to engineer the comparable combination is crucial for high-efficiency performance. To avoid underperformance of the nitrogen fixation cell, a robust yet continuous energy source is desired.

Hydropower

Hydropower is a sustainable and renewable energy source, massively stored in falling water, flowing rivers, and even marine environments, and is a promising energy source for sustainable and flexible energy generation. Therefore, a hydropower-driven TENG has been considered to be a promising energy source for nitrogen fixation. With the substantial advantages of hydropower, such as its high abundance on earth, periodic movements, and ease of acquisition, a TENG driven by hydropower would be a promising foundation for nitrogen fixation. Xie *et al.* exploited the merits of the disk-based sliding TENG because most types of irregular motion can be converted into rotational mechanical energy and applied for electricity generation.[67] Hydropower is a representatively irregular motion with ungovernable directions and strength, which allows a wide
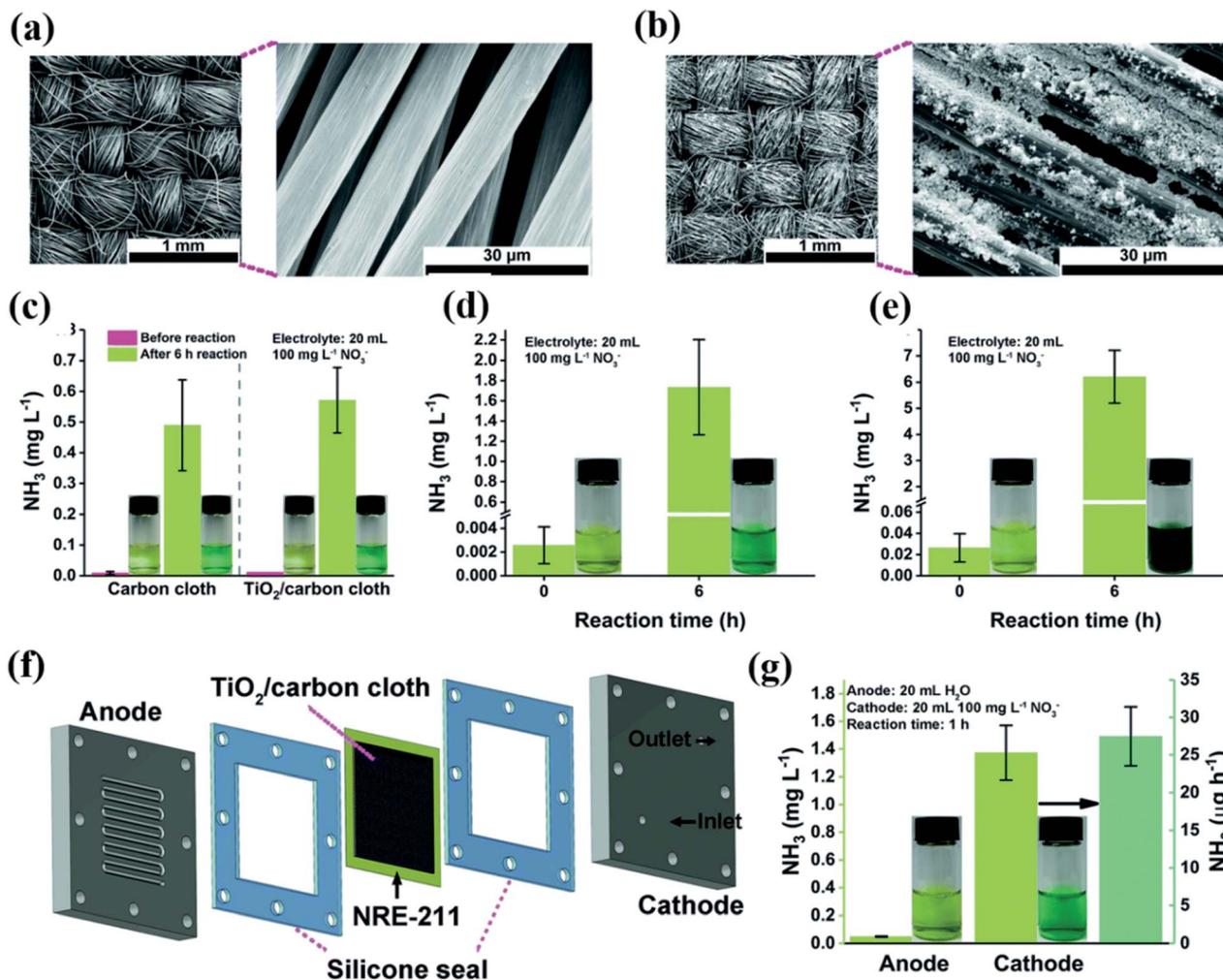
19512 | *J. Mater. Chem. A*, 2022, **10**, 19506–19517

This journal is © The Royal Society of Chemistry 2022

Fig. 4 (a) SEM images of carbon cloth and (b) TiO_2 modified carbon cloth. Concentration variations of NH_3 using 100 mg L^{-1} NO_3^- as electrolyte in a single cell with (c) DC power (−3 V), (d) a rectified TENG-2 drive and (e) an electromagnetic transformer step-down (350 : 12) and rectified TENG-2 drive. (f) Schematic graphs of the dual-compartment electrocatalytic cell. (g) Concentration and mass yield per hour of NH_3 in a dual-compartment electrochemical cell with voltage step-down (350 : 4) and rectified TENG-2 drive. Reproduced with permission.[60] Copyright 2020, Royal Society of Chemistry.

application of the sliding TENG with configuration variations.[68,69] Moreover, the disk-based structure is also a favorable infrastructure for multi-layer integration and parallel connection that enables the expansion of energy harvesting capacity. This TENG device driven by water can obtain an instantaneous peak voltage of 470 V and a peak current of 90.6 mA m^{-2}. Zhao et al.[33] also proposed a networked integrated TENG that can produce electric power of 1.03 mW with an area of 100 × 70 mm^2.

The "blue power"-triggered TENGs can easily serve as the energy component for self-powered seawater desalination and water disinfection systems. In 2013, a contact-separation TENG was fabricated using printing circuit technology with four clamped chambers powered by the TENG device for electrodialysis desalination. The salt solution can be desalinated to drinking water after 16 h with a 98.5% desalination rate. Additionally, this process produces hydrogen at a rate of 2.8 × 10^{-8} L s^{-1}.[70] For water disinfection, Tian et al. reported

a spherical TENG that collects water wave energy in which the open-circuit voltage can reach 50 V. The electricity converted from wave motions is utilized to power the disinfection device of two carbon cloth electrodes deposited with ZnO nanowires. When model bacteria flow through the device, all tested bacteria are completely inactivated. The inactivation performance was even retained for 20 minutes after the TENG was disconnected.[71]

Wind

Wind is also a naturally-existing energy source used for triboelectric nanogenerators. Compared with conventional approaches, which use the electromagnetic effect based on a turbine, TENG possesses the advantages of being low-cost, scalable and easily fabricated.[35,72] TENGs driven by wind are also widely applied in electric device powering or as an electricity producer for energy storage equipment. The practical

This journal is © The Royal Society of Chemistry 2022

J. Mater. Chem. A, 2022, **10**, 19506–19517 | **19513**

utilization of wind-driven TENGs puts forward a prescription for the photochemical and electrochemical decomposition of CO_2 and gaseous acetaldehyde. Li *et al.* suggest that TENG-generated high voltage electricity can directly break down the gas and produce plasma. The high-energy electrons can subsequently react with CO_2, forming highly reactive CO_2^- anions, efficiently improving the decomposition efficiency at room temperature with a wind speed of 4.7 m s^{-1}.[73] In work reported by Fu, a piston-based triboelectric nanogenerator (P-TENG) is combined with a photocatalytic reactor and the acetaldehyde removal rate of the system reached 63% within 30 min.[74] In addition to these examples, TENGs show a wide range of applications in antibiotics degradation,[75] wastewater treatment[23] and other organic pollutant treatments.[76,77]

Human motion

Besides the rational selection of mechanical energy sources, elevating the sensitivity of TENG devices is also an important approach to achieving excellent energy scavenging. Recently, soft TENGs that can be triggered by a weak deformation, such as cloth folding or bending, have expanded the application scenarios of TENGs.[78] However, due to the limited content, only a simple introduction of the features and advantages of soft TENGs is involved in this report. Soft TENGs normally function in contact-separation mode or sliding mode; due to the soft characteristic, more sufficient contact can be realized. With compact contact, the contact area of the interface is increased due to the soft characteristic. Also, the super stretchable and lightweight TENG devices can adhere to multiple surfaces, such as a moving wrist or hand. The soft TENG is also able to undergo various deformations and retain a stable operation property. The collected electricity can be stored in batteries or wireless charging transmitters for further utilization.

Integration with solar cells

In fact, aside from improvements to the energy output by modifying the sensitivity and structural design, TENG has been a hybridized energy supply for water splitting with solar energy since its development.[79] Similar to the preliminary constituents of the nitrogen fixation system, a hybridized water-driven TENG and water splitting cell was surveyed in 2014.[80] The subsequent collaboration with solar energy revealed that the combination of the TENG potency and the photoelectrochemical (PEC) NH_3 synthesis significantly improves the output efficiency. Even though the results suggest that the direct electrolysis of water can be triggered by the high rotation speed of a TENG, a similar peak current can also be achieved with the assistance of illumination under a relatively lower rotation speed.[81,82] The coupling effect of PEC and TENG leads to an improved yield rate. Inspired by this, PEC NH_3 synthesis with a TENG energy supply can be an alternative pathway for improving nitrogen fixation efficiency. It has been proved by several works that efficient PEC NH_3 synthesis can be achieved by introducing the appropriate photoanode, catalysis, and photocathode.[83,84] With the external TENG energy supply, not only can the PEC efficiency be excessively enhanced, but the functional availability

also breaks the PEC limitations of working in a dark environment. In addition, the hybridized system can also employ wind as the energy source for applications in wider realms.[85] It also indicates the bright future of integrating nitrogen fixation systems with vast energy sources in the ambient environment.

Catalyst strategy

The previous sections show the improvement of TENG performance and the evolution of electrocatalytic sections, from a single cell to dual-compartment, from steel needles to TiO_2 modified carbon cloth. As is known, the electrocatalytic nitrogen reduction reaction (NRR) has been a promising process for replacing the Haber–Bosch process and thus many studies have been conducted to search for efficient strategies to improve NRR efficiency. For integration with a TENG energy supply, the electrocatalytic reaction components need to be capable of low energy consumption and easy fabrication. Wang *et al.* introduced a new class of glassy porous M–Te (M = Ru, Rh, Ir) nanorods that are considered to be excellent electrocatalysts for NRR.[86] These $IrTe_4$ porous nanorods (PNRs), fabricated by a unique method, show a strong ability to be involved in reactions. The linear sweeping voltammetry (LSV) results indicate an obvious increase in production using $IrTe_4$ compared with $RuTe_4$ or $RhTe_4$ PNRs. The work also compared the Faraday efficiency (FE) of $IrTe_2$ and $IrTe_8$ PNRs, which both show inferior performance compared to that of $IrTe_4$. Due to Ir favoring the competitive adsorption of hydrogen species, FE_{NH_3} exhibits a strong decrease when more Ir is introduced and FE_{H_2} shows an adverse variation. Although the scanning transmission electron microscopy-energy-dispersive X-ray spectroscopy (STEM-EDS) elemental mapping of $IrTe_4$ PNRs shows a homogeneous distribution of Ir and Te, the catalysis performance of glassy $IrTe_4$ indicates a strong enhancement when compared with crystalline $IrTe_4$ because of the abundant dangling bonds. According to density functional theory (DFT), $IrTe_4$ possesses the lowest d-band center and stronger mixing of anti-bonding and bonding orbitals near the Fermi level. From the analysis, it can be determined that Ir functions as a strong attractor for H_2O and dissociates the H–O bond while Te functions as the electron supplier for nitrogen. The optimal $IrTe_4$ is capable of FE and NH_3 yield rates of 15.3% and 51.1 μg h^{-1} mg$_{cat}$$^{-1}$. The yield of $IrTe_4$ shows a trend from small to large with the increase of electrolysis time, indicating the stability of $IrTe_4$ PNRs. Unfortunately, the reaction with $IrTe_4$ needs a high temperature of 440 °C, which is currently difficult for TENG devices to achieve. However, a recently reported study[87] shows that the output performance of a DC-TENG can be enhanced by three orders of magnitude at a higher working temperature because employing a higher temperature can simultaneously enhance the triboelectric charge density and the electrostatic breakdown. This finding demonstrates that mechanical and thermal energy can be harvested simultaneously when the TENG operates at a higher temperature, which in turn offsets the required catalytic energy consumption.

Besides the unique synthesis method, there are also generally applicable surface modification methods for improving the

19514 | *J. Mater. Chem. A*, 2022, **10**, 19506–19517

This journal is © The Royal Society of Chemistry 2022

yield rate of NRR. For instance, with a surface chalcogenation strategy, the NH$_3$ yield rate can increase by 16 times.[88] Ling *et al.*[89] and Qi *et al.*[90] both introduce the boron (B) atom to decorate a metal-free single atom photocatalyst or synthesize transition metal boride monolayer catalysts. Electrocatalysts that function at room temperature and atmospheric pressure have also been investigated.[91,92] Due to advanced electroactivity to activate the inert molecules, the atomic catalysts are also promising selections to investigate their potential in nitrogen fixations.[97,99] Combined with optimized TENGs, a self-powered high fixation-efficiency system can be achieved through continuous efforts.

Perspective

As described in the previous sections, we can conclude that the conjunction of a TENG device with a nitrogen reduction cell is an unprecedented opportunity to obtain a novel and feasible method for nitrogen fixation. Limited by the large energy consumption of the Haber–Bosch process, nitrogen fixation industries cannot widely develop in the world. However, TENG is a sustainable green energy generator with simple fabrication, low cost, and small volume, especially in the low-frequency range, making it a suitable energy harvester in a wide range of fields. Moreover, advanced manufacturing technology and surface modification enable a sufficient energy output, which reached 7.6 W m^{-2} in the latest report.[93] DC output is normally preferred for sufficient NO$_3^-$ production, so TENG is a favorable energy harvester as it is capable of converting AC into DC. By utilizing mechanical rectifiers or phase control, DC current can be easily acquired. Moreover, Zhang *et al.* reported a DC-TENG based on rotational motions with a reversible joining of the electrodes to the external circuit from which a DC output can be accomplished. To further decrease the crest factor and achieve a constant DC, some researchers have also reported methods of phase control to convert mechanical energy into DC. In addition to external applied equipment or structural modification, DC TENG output can also arise from dielectric breakdown.[94] These methods provide a new paradigm to create DC-TENGs to directly power electronic devices.

As mentioned in previous sections, TENGs are capable of high voltage and low current which can be utilized to enhance nitrogen reduction efficiency. Realistic applications of nitrogen fixation require large amounts of energy and integrated TENG networks and hybridized functional units show a promising future. Distributed sustainable nitrogen reduction also exhibits opportunities due to the characteristics of TENGs. In developing counties, typical fertilizer usage is much less than the global average.[95] This can cause poverty and hunger and can even impede economic development. In countries which struggle with insufficient fertilizer production, TENG systems enable the wide employment of distributed and sustainable nitrogen reduction units for small-scale and flexible fertilizer production. However, during the investigation, we found several limitations restricting the development of the TENG-based nitrogen fixation system. First, the confined application range keeps most of the studies at the experimental level; although some researchers have tried to integrate experimental results with theoretical assumptions[96] to further optimize their works, the conversion efficiency cannot be fully verified. The second issue is the unpredictability of mechanical energy sources, which makes it more imperative and indispensable to enhance the energy harvesting efficiency of TENG devices.

We have also presented several works concerning novel catalysts for nitrogen reduction. Multiple works have dispensed with the limitation of high temperature, realizing operation in an ambient environment with natural airflow as the energy source. Based on these works, we propose that the integration of TENG and nitrogen reduction as a self-powered sustainable N$_2$ fixation system will be a highly competitive green solution for the fertilizer industry. We also propose that active research and continuous efforts in this field will benefit the solution of emerging challenges in the nitrogen cycle. Further studies can assist in the improvement of integration strategies and widen the application scope of the hybridized TENG and nitrogen fixation system.

Conflicts of interest

There are no conflicts to declare.

Acknowledgements

Notes and references

1 H. Volland, *Handbook of Atmospheric Electrodynamics*, CRC Press, 1995.
2 Y. Li, F. Pan and H. Yao, *J. Soils Sediments*, 2019, **19**, 1948–1958.
3 X. Xue, R. Chen, C. Yan, P. Zhao, Y. Hu, W. Zhang, S. Yang and Z. Jin, *Nano Res.*, 2019, **12**, 1229–1249.
4 K. Miki, M. Panesi, E. Prudencio and S. Prudhomme, *Phys. Plasmas*, 2012, **19**, 023507.
5 A. S. Travis, *The Synthetic Nitrogen Industry in World War I: Its Emergence and Expansion*, Springer, 2015.
6 A. S. Travis*The Synthetic Nitrogen Industry in World War I*, Springer, 2015, pp. 17–72.
7 B. Wang, T. Dong, A. Myrlie, L. Gu, H. Zhu, W. Xiong, P. Maness, R. Zhou and J. Yu, *Green Chem.*, 2019, **21**, 2928–2937.
8 S. Li, J. A. Medrano, V. Hessel and F. Gallucci, *Processes*, 2018, **6**, 248.
9 J. W. Erisman, M. A. Sutton, J. Galloway, Z. Klimont and W. Winiwarter, *Nat. Geosci.*, 2008, **1**, 636–639.

10 J. N. Galloway, A. R. Townsend, J. W. Erisman, M. Bekunda, Z. Cai, J. R. Freney, L. A. Martinelli, S. P. Seitzinger and M. A. Sutton, *Science*, 2008, **320**, 889–892.

11 T. Balser, *Tales from the Underground: A Natural History of Subterranean Life*, Basic Books, New York, 2001.

12 V. Kyriakou, I. Garagounis, A. Vourros, E. Vasileiou and M. Stoukides, *Joule*, 2020, **4**, 142–158.

13 X. Cui, C. Tang and Q. Zhang, *Adv. Energy Mater.*, 2018, **8**, 1800369.

14 I. A. Amar, R. Lan, C. T. Petit and S. Tao, *J. Solid State Electrochem.*, 2011, **15**, 1845–1860.

15 S. Gao, Y. Zhu, Y. Chen, M. Tian, Y. Yang, T. Jiang and Z. L. Wang, *Mater. Today*, 2019, **28**, 17–24.

16 R. Zhang and H. Olin, *EcoMat*, 2020, **2**, e12062.

17 G. Deng, T. Wang, A. A. Alshehri, K. A. Alzahrani, Y. Wang, H. Ye, Y. Luo and X. Sun, *J. Mater. Chem. A*, 2019, **7**, 21674–21677.

18 S. Liu, S. Yin, S. Jiao, H. Zhang, Z. Wang, Y. Xu, X. Li, L. Wang and H. Wang, *Mater. Today Energy*, 2021, 100828.

19 C. Yang, B. Huang, S. Bai, Y. Feng, Q. Shao and X. Huang, *Adv. Mater.*, 2020, **32**, 2001267.

20 M. I. Ahmed, C. Liu, Y. Zhao, W. Ren, X. Chen, S. Chen and C. Zhao, *Angew. Chem., Int. Ed.*, 2020, **59**, 21465–21469.

21 Z. L. Wang, *Mater. Today*, 2017, **20**, 74–82.

22 F.-R. Fan, Z.-Q. Tian and Z. L. Wang, *Nano Energy*, 2012, **1**, 328–334.

23 S. Chen, N. Wang, L. Ma, T. Li, M. Willander, Y. Jie, X. Cao and Z. L. Wang, *Adv. Energy Mater.*, 2016, **6**, 1501778.

24 X. Pu, L. Li, H. Song, C. Du, Z. Zhao, C. Jiang, G. Cao, W. Hu and Z. L. Wang, *Adv. Mater.*, 2015, **27**, 2472–2478.

25 Y. Zi, J. Wang, S. Wang, S. Li, Z. Wen, H. Guo and Z. L. Wang, *Nat. Commun.*, 2016, **7**, 1–8.

26 Y. Zi, H. Guo, Z. Wen, M.-H. Yeh, C. Hu and Z. L. Wang, *ACS Nano*, 2016, **10**, 4797–4805.

27 J. Chen, J. Yang, Z. Li, X. Fan, Y. Zi, Q. Jing, H. Guo, Z. Wen, K. C. Pradel and S. Niu, *ACS Nano*, 2015, **9**, 3324–3331.

28 Z. Yuan, C. Wang, J. Xi, X. Han, J. Li, S.-T. Han, W. Gao and C. Pan, *ACS Energy Lett.*, 2021, **6**, 2809–2816.

29 A. Matin Nazar, K.-J. Idala Egbe, A. Abdollahi and M. A. Hariri-Ardebili, *Energies*, 2021, **14**, 5600.

30 D. Hao, D. Liu, S. Gao, H. Arandiyan, X. Bai, Q. Kong, W. Wei, P. K. Shen and B.-J. Ni, *Mater. Today*, 2021, **46**, 212–233.

31 *World Fertilizer Trends and Outlook to 2020*, FAO-Food and Agriculture Organization, United Nations, 2017.

32 C. Smith, A. K. Hill and L. Torrente-Murciano, *Energy Environ. Sci.*, 2020, **13**, 331–344.

33 X. J. Zhao, S. Y. Kuang, Z. L. Wang and G. Zhu, *ACS Nano*, 2018, **12**, 4280–4285.

34 K. Dong, Z. Wu, J. Deng, A. C. Wang, H. Zou, C. Chen, D. Hu, B. Gu, B. Sun and Z. L. Wang, *Adv. Mater.*, 2018, **30**, 1804944.

35 B. Chen, Y. Yang and Z. L. Wang, *Adv. Energy Mater.*, 2018, **8**, 1702649.

36 L. Zhang, B. Zhang, J. Chen, L. Jin, W. Deng, J. Tang, H. Zhang, H. Pan, M. Zhu and W. Yang, *Adv. Mater.*, 2016, **28**, 1650–1656.

37 X. Chen, J. Xiong, K. Parida, M. Guo, C. Wang, C. Wang, X. Li, J. Shao and P. S. Lee, *Nano Energy*, 2019, **64**, 103904.

38 M. C. Wong, W. Xu and J. Hao, *Adv. Funct. Mater.*, 2019, **29**, 1904090.

39 X. Wang, S. Wang, Y. Yang and Z. L. Wang, *ACS Nano*, 2015, **9**, 4553–4562.

40 W. Tang, C. B. Han, C. Zhang and Z. L. Wang, *Nano Energy*, 2014, **9**, 121–127.

41 D. Gao, X. Zhang, B. Chong, G. Xiao and D. Tian, *Phys. Chem. Chem. Phys.*, 2017, **19**, 4288–4296.

42 J. Yang, J. Chen, Y. Liu, W. Yang, Y. Su and Z. L. Wang, *ACS Nano*, 2014, **8**, 2649–2657.

43 B. Meng, X. Cheng, X. Zhang, M. Han, W. Liu and H. Zhang, *Appl. Phys. Lett.*, 2014, **104**, 103904.

44 B. Dudem, N. D. Huynh, W. Kim, D. H. Kim, H. J. Hwang, D. Choi and J. S. Yu, *Nano Energy*, 2017, **42**, 269–281.

45 W. Yang, J. Chen, X. Wen, Q. Jing, J. Yang, Y. Su, G. Zhu, W. Wu and Z. L. Wang, *ACS Appl. Mater. Interfaces*, 2014, **6**, 7479–7484.

46 X. Pu, H. Guo, J. Chen, X. Wang, Y. Xi, C. Hu and Z. L. Wang, *Sci. Adv.*, 2017, **3**, e1700694.

47 S. Wang, S. Niu, J. Yang, L. Lin and Z. L. Wang, *ACS Nano*, 2014, **8**, 12004–12013.

48 Q. Zheng, B. Shi, F. Fan, X. Wang, L. Yan, W. Yuan, S. Wang, H. Liu, Z. Li and Z. L. Wang, *Adv. Mater.*, 2014, **26**, 5851–5856.

49 S. Cheon, H. Kang, H. Kim, Y. Son, J. Y. Lee, H. J. Shin, S. W. Kim and J. H. Cho, *Adv. Funct. Mater.*, 2018, **28**, 1703778.

50 Y. Yang, H. Zhang, X. Zhong, F. Yi, R. Yu, Y. Zhang and Z. L. Wang, *ACS Appl. Mater. Interfaces*, 2014, **6**, 3680–3688.

51 J. Zhang, Y. Zheng, L. Xu and D. Wang, *Nano Energy*, 2020, **69**, 104435.

52 S. Kim, M. K. Gupta, K. Y. Lee, A. Sohn, T. Y. Kim, K. S. Shin, D. Kim, S. K. Kim, K. H. Lee and H. J. Shin, *Adv. Mater.*, 2014, **26**, 3918–3925.

53 G. Liu, J. Nie, C. Han, T. Jiang, Z. Yang, Y. Pang, L. Xu, T. Guo, T. Bu and C. Zhang, *ACS Appl. Mater. Interfaces*, 2018, **10**, 7126–7133.

54 G. Zhu, J. Chen, Y. Liu, P. Bai, Y. S. Zhou, Q. Jing, C. Pan and Z. L. Wang, *Nano Lett.*, 2013, **13**, 2282–2289.

55 Z. Lin, J. Chen, X. Li, Z. Zhou, K. Meng, W. Wei, J. Yang and Z. L. Wang, *ACS Nano*, 2017, **11**, 8830–8837.

56 W.-S. Jung, M.-G. Kang, H. G. Moon, S.-H. Baek, S.-J. Yoon, Z.-L. Wang, S.-W. Kim and C.-Y. Kang, *Sci. Rep.*, 2015, **5**, 1–6.

57 Z. Quan, C. B. Han, T. Jiang and Z. L. Wang, *Adv. Energy Mater.*, 2016, **6**, 1501799.

58 C. Qian, L. Li, M. Gao, H. Yang, Z. Cai, B. Chen, Z. Xiang, Z. Zhang and Y. Song, *Nano Energy*, 2019, **63**, 103885.

59 S.-B. Jeon, D. Kim, G.-W. Yoon, J.-B. Yoon and Y.-K. Choi, *Nano Energy*, 2015, **12**, 636–645.

60 I. S. Bayer, F. Brandi, R. Cingolani and A. Athanassiou, *Colloid Polym. Sci.*, 2013, **291**, 367–373.

61 D. Kim, I.-W. Tcho, I. K. Jin, S.-J. Park, S.-B. Jeon, W.-G. Kim, H.-S. Cho, H.-S. Lee, S. C. Jeoung and Y.-K. Choi, *Nano Energy*, 2017, **35**, 379–386.

62 C. Jiang, X. Li, Y. Yao, L. Lan, Y. Shao, F. Zhao, Y. Ying and J. Ping, *Nano Energy*, 2019, **66**, 104121.

63 S.-J. Park, M.-L. Seol, S.-B. Jeon, D. Kim, D. Lee and Y.-K. Choi, *Sci. Rep.*, 2015, **5**, 1–7.

64 S. Gao, Y. Zhu, Y. Chen, M. Tian, Y. Yang, T. Jiang and Z. L. Wang, *Mater. Today*, 2019, **28**, 17–24.

65 K. Han, J. Luo, Y. Feng, L. Xu, W. Tang and Z. L. Wang, *Energy Environ. Sci.*, 2020, **13**, 2450–2458.

66 S. Wang, Y. Xie, S. Niu, L. Lin and Z. L. Wang, *Adv. Mater.*, 2014, **26**, 2818–2824.

67 Y. Xie, S. Wang, S. Niu, L. Lin, Q. Jing, Y. Su, Z. Wu and Z. L. Wang, *Nano Energy*, 2014, **6**, 129–136.

68 X. Wang, S. Niu, Y. Yin, F. Yi, Z. You and Z. L. Wang, *Adv. Energy Mater.*, 2015, **5**, 1501467.

69 Y. Xi, H. Guo, Y. Zi, X. Li, J. Wang, J. Deng, S. Li, C. Hu, X. Cao and Z. L. Wang, *Adv. Energy Mater.*, 2017, **7**, 1602397.

70 Y. Yang, H. Zhang, Z.-H. Lin, Y. Liu, J. Chen, Z. Lin, Y. S. Zhou, C. P. Wong and Z. L. Wang, *Energy Environ. Sci.*, 2013, **6**, 2429–2434.

71 J. Tian, H. Feng, L. Yan, M. Yu, H. Ouyang, H. Li, W. Jiang, Y. Jin, G. Zhu and Z. Li, *Nano Energy*, 2017, **36**, 241–249.

72 Y. Yang, G. Zhu, H. Zhang, J. Chen, X. Zhong, Z.-H. Lin, Y. Su, P. Bai, X. Wen and Z. L. Wang, *ACS Nano*, 2013, **7**, 9461–9468.

73 S. Li, B. Zhang, G. Gu, X. Xiang, W. Zhang, X. Shi, K. Zhao, Y. Zhu, J. Guo and P. Cui, *Nano Energy*, 2021, **88**, 106287.

74 Q. Fu, Y. Liu, J. Mo, Y. Lu, C. Cai, Z. Zhao, S. Wang and S. Nie, *ACS Nano*, 2021, **15**, 10577–10586.

75 J. Mo, Y. Liu, Q. Fu, C. Cai, Y. Lu, W. Wu, Z. Zhao, H. Song, S. Wang and S. Nie, *Nano Energy*, 2022, **93**, 106842.

76 S. Gao, Y. Chen, J. Su, M. Wang, X. Wei, T. Jiang and Z. L. Wang, *ACS Nano*, 2017, **11**, 3965–3972.

77 S. O. Ganiyu, C. A. Martinez-Huitle and M. A. Rodrigo, *Appl. Catal., B*, 2020, **270**, 118857.

78 Y. Song, N. Wang, C. Hu, Z. L. Wang and Y. Yang, *Nano Energy*, 2021, 105919.

79 L. Jin, B. Zhang, L. Zhang and W. Yang, *Nano Energy*, 2019, **66**, 104086.

80 W. Tang, Y. Han, C. B. Han, C. Z. Gao, X. Cao and Z. L. Wang, *Adv. Mater.*, 2015, **27**, 272–276.

81 A. Wei, X. Xie, Z. Wen, H. Zheng, H. Lan, H. Shao, X. Sun, J. Zhong and S.-T. Lee, *ACS Nano*, 2018, **12**, 8625–8632.

82 X. Wei, Z. Wen, Y. Liu, N. Zhai, A. Wei, K. Feng, G. Yuan, J. Zhong, Y. Qiang and X. Sun, *Nano-Micro Lett.*, 2020, **12**, 1–10.

83 W. Wang, S. Zhang, Y. Liu, L.-R. Zheng, G. Wang, Y. Zhang, H. Zhang and H. Zhao, *Chin. Chem. Lett.*, 2021, **32**, 805–810.

84 W. Ye, M. Arif, X. Fang, M. A. Mushtaq, X. Chen and D. Yan, *ACS Appl. Mater. Interfaces*, 2019, **11**, 28809–28817.

85 X. Ren, H. Fan, C. Wang, J. Ma, H. Li, M. Zhang, S. Lei and W. Wang, *Nano energy*, 2018, **50**, 562–570.

86 J. Wang, B. Huang, Y. Ji, M. Sun, T. Wu, R. Yin, X. Zhu, Y. Li, Q. Shao and X. Huang, *Adv. Mater.*, 2020, **32**, 1907112.

87 D. Liu, L. Zhou, S. Li, Z. Zhao, X. Yin, Z. Yi, C. Zhang, X. Li, J. Wang and Z. L. Wang, *Adv. Mater. Technol.*, 2020, **5**, 2000289.

88 C. Yang, B. Huang, S. Bai, Y. Feng, Q. Shao and X. Huang, *Adv. Mater.*, 2020, **32**, 2001267.

89 C. Ling, X. Niu, Q. Li, A. Du and J. Wang, *J. Am. Chem. Soc.*, 2018, **140**, 14161–14168.

90 S. Qi, Y. Fan, L. Zhao, W. Li and M. Zhao, *Appl. Surf. Sci.*, 2021, **536**, 147742.

91 D. Bao, Q. Zhang, F. L. Meng, H. X. Zhong, M. M. Shi, Y. Zhang, J. M. Yan, Q. Jiang and X. B. Zhang, *Adv. Mater.*, 2017, **29**, 1604799.

92 J. Han, Z. Liu, Y. Ma, G. Cui, F. Xie, F. Wang, Y. Wu, S. Gao, Y. Xu and X. Sun, *Nano Energy*, 2018, **52**, 264–270.

93 S. S. Rana, M. T. Rahman, S. Sharma, M. Salauddin, S. H. Yoon, C. Park, P. Maharjan, T. Bhatta and J. Y. Park, *Nano Energy*, 2021, **88**, 106300.

94 D. Liu, L. Zhou, Z. L. Wang and J. Wang, *iScience*, 2021, 102018.

95 I. J. Minde, T. S. Jayne, E. W. Crawford, J. Ariga and J. Govereh, *Promoting Fertilizer Use in Africa: Current Issues and Empirical Evidence from Malawi, Zambia, and Kenya*, 2008.

96 K. Han, J. Luo, J. Chen, B. Chen, L. Xu, Y. Feng, W. Tang and Z. L. Wang, *Microsyst. Nanoeng.*, 2021, **7**, 1–8.

97 M. Sun, H. H. Wong, T. Wu, A. W. Dougherty and B. Huang, Entanglement of Spatial and Energy Segmentation for C_1 Pathways in CO_2 Reduction on Carbon Skeleton Supported Atomic Catalysts, *Adv. Energy Mater.*, 2022, **12**, 2103781.

98 J. Liu, Z. Wei, Y. Dou, Y. Feng and J. Ma, Ru-doped phosphorene for electrochemical ammonia synthesis, *Rare Met.*, 2020, **39**, 874–880.

99 Z. Wei, Y. Zhu, J. Liu, Z. Zhang, W. Hu, H. Xu, Y. Feng and J. Ma, Recent advance in single-atom catalysis, *Rare Met.*, 2021, **40**, 767–789.

This journal is © The Royal Society of Chemistry 2022

J. Mater. Chem. A, 2022, **10**, 19506–19517 | **19517**